Geochemical discrimination of Early Palaeogene bauxites in Croatia

Erli Kovačević Galović, Nikolina Ilijanić, Zoran Peh, Slobodan Miko and Ozren Hasan

Croatian Geological Survey, Sachsova 2, P.O. Box 268, HR-10000 Zagreb, Croatia;
(corresponding author: ekovacevic@hgi-cgs.hr)

Geologia Croatica

ABSTRACT

Two discriminant function models were created in order to distinguish between major- and trace-element geochemical patterns typical of Lower Palaeogene (Palaeocene, Pc) bauxites formed on the portion of the carbonate platform comprising the Karst or External Dinarides. Four groups of bauxites from Istria, North Adriatic Islands, North Dalmatia and Central Dalmatia have been distinguished, according to their specific combinations of major and trace elements, characteristic conditions of formation, and processes prevailing in the karst environment during subaerial exposure of the carbonate platform. Typically, in both models the first discriminant function explains most of the system variability. However, the trace-element model proves itself as a more helpful predictive tool, representing the straightforward example of classification of the samples into four pre-defined groups of Pc bauxites. Generally, both models follow a characteristic trend in geochemical signature related to the recent geographical position of the bauxite deposits, namely a decrease in K_2O and an increase in the Cr content in a SE direction (from Istria to Dalmatia). This was most probably the result of environmental conditions during the AdCP Cretaceous-Palaeogene emergent stage (Istria), and emplacement of parent rocks (ophiolite belt) supplying the necessary material for bauxite genesis (Central Dalmatia).

Keywords: Bauxite; Adriatic Carbonate platform; Dinarides; Geochemistry; Discriminant function model

1. INTRODUCTION

Unlike many other types of ores and raw materials, bauxites were for a long time treated only as an aluminum ore, with all research efforts focused on the assessment of conditions of their detection, exploitation and refinement. In spite of a great number of mineralogical and chemical analyses (albeit only partial in most cases), from bauxite deposits and occurrences in Croatia being available in various studies and professional reports, bauxite genesis, particularly in relation to the adjacent karst (palaeo)environment and its tectonostratigraphic constraints, was largely underestimated. Only lately, have models of the orogenic evolution of the Adriatic (Adriatic–Dinaric) Carbonate Platform (AdCP) with special reference to External Dinarides of the NE Adriatic region underlined the importance of a number of hiatuses of variable duration marked by bauxitic deposits (VLAHOVIĆ et al., 2005; KORBAR, 2009). Since bauxites are now well recog-

nized as tectonic and climatic event markers at regional unconformities, these investigations call for additional correlative studies within and across different stratigraphic horizons, bearing in mind that clearly expressed emergent surfaces set the stage for the resonant interplay of tectonics, volcanism, eustasy and climate on various parts of the carbonate platform (D'ARGENIO & MINDSZENTY, 1995). Such a complex bauxite research seems indispensable in the light of the new lithostratigraphic scheme that became the basis for regional correlation studies within the entire region of the Croatian Karst Dinarides during the last two decades (e.g. MATIČEC et al., 1996; TIŠLJAR et al., 2002; VLAHOVIĆ et al., 2002; DRAGIČEVIĆ & VELIĆ, 2002). The amassed data in the plentiful literature on Croatian bauxites (e.g. ŠINKOVEC, 1973; SAKAČ et al., 1987; ŠINKOVEC & SAKAČ, 1981; ŠUŠNJARA et al., 1990; SAKAČ et al., 1984; ŠINKOVEC et al., 1994) is largely confined within the limits of particular deposits, stratigraphic horizons, or local unconformities,

but has immense potential indispensable in building regional models of platform evolution, except for rarer works addressing a wider scope (e.g. SAKAČ & ŠINKOVEC, 1991).

Croatian bauxites are hosted in carbonate rocks marking regional unconformities between several stratigraphic levels, of which the Upper Cretaceous – Lower Palaeogene hiatus can be singled out as a major one. In some parts of the AdCP (Istrian karst) emergence was uncharacteristically long, from as far back as the Lower Cretaceous (MATIČEC et al., 1996; Croatian Geological Survey, 2009), while elsewhere it was much shorter. The extent of subaerial exposure during the stratigraphic gaps is of particular importance in understanding the origin of bauxites, which is why the geochemical and mineralogical signature has much to say about the intervening processes prevailing on the emergent carbonate platform. The Lower Palaeogene (Palaeocene, Pc) bauxites are specifically targeted for this purpose owing to their variable time span of emplacement (Lower Cretaceous to Lower Eocene) within the AdCP (from NE to SE), and assumed differences in geochemical signal received during exposure. Accordingly, the main purpose of this investigation was to assess the geochemical contrast (aided by qualitative mineralogical analysis) among the different groups of Pc bauxites previously defined in relation to their palaeographical/palaeotectonic settings (Fig. 1) To this effect, a multivariate statistical assessment of a primary geochemical pattern dis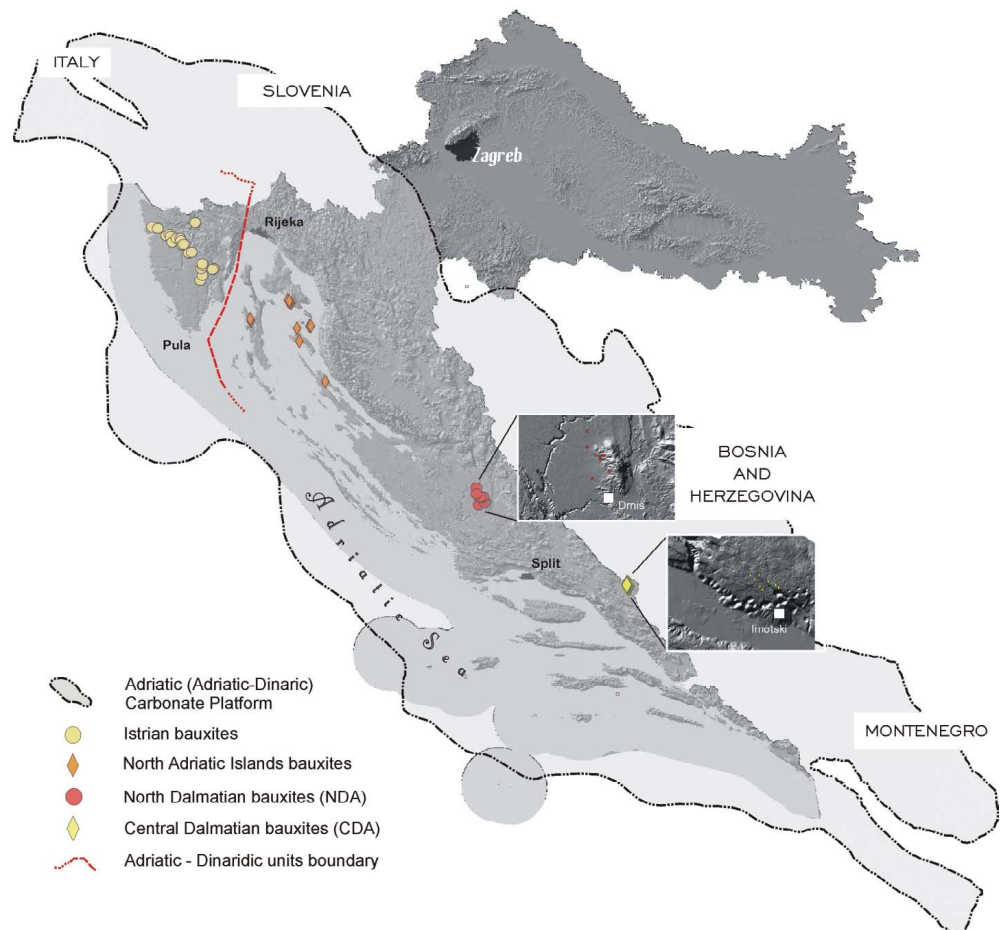tinguishing between samples from Istria, the North Adriatic islands, North Dalmatia (Drniš area) and Central Dalmatia (Imotski area) was performed, preferring multiple discriminant analysis (MDA) as the most helpful mathematical tool. The latter is employed as a method of data reduction and organization which offers a quick, simple and effective means of clarifying significant groupings and trends among environmentally distinct sediment samples, in this case solely on the basis of their geochemical composition.

2. MATERIALS AND METHODS

2.1. Geological setting

The area of the Croatian Karst (External or Outer) Dinarides is a thick carbonate succession deposited from the Middle Permian (or even Upper Carboniferous) to the Eocene on platforms of different ages, type and palaeogeographical setting. The evolution of the Karst Dinarides area started on an epeiric carbonate platform along the northern Gondwana margin with a significant deposition of mixed carbonate-siliciclastic sediments in the Permian, and mostly siliciclastic deposits in the Early Triassic (VLAHOVIĆ et al., 2002). In the Middle Triassic, steep faults formed in the basement and separation of the Adria Microplate occurred, characterized by carbonate facies with locally significant volcaniclastic influence. A Late Triassic succession of Hauptdolomite and Dachstein limestones represents typical deposits of the huge isolated Southern Tethyan Megaplatform (VLAHOVIĆ et

Figure 1: Shaded relief map of Croatia with superimposed area showing the recent distribution of Adriatic (Adriatic-Dinaric) Carbonate Platform (compiled from VLAHOVIĆ et al., 2005) and locations of sampled Early Palaeogene bauxites. Border between the Adriatic and Dinaric units inferred (partly) after KORBAR, 2009.

Adriatic (Adriatic-Dinaric) Carbonate Platform
Istrian bauxites
North Adriatic Islands bauxites
North Dalmatian bauxites (NDA)
Central Dalmatian bauxites (CDA)
Adriatic - Dinaridic units boundary

al., 2005). During the Late Liassic, it was dissected into smaller carbonate platforms, resulting in formation of the Adriatic Basin, with the Adriatic Carbonate Platform (AdCP) along its eastern side. This was marked by predominantly shallow-marine deposition, but a combination of synsedimentary tectonics and eustatic changes resulted in frequent emersions of variable duration, characterized by local deposition of bauxites. According to other authors (KORBAR, 2009, and references therein), two carbonate platforms (Adriatic and Dinaric), separated by the inter-platform Budva-Cukali basin, were formed instead of the single AdCP. These were used as a basis for a new model of the Mesozoic–Cenozoic evolution of the region and further divided into four tectonostratigraphic units: Dinaridic NE unit (Inner Karst), Dinaridic SW unit (High Karst), Adriatic NE unit (Dalmatian Karst) and Adriatic SW unit (Istrian Karst). Disintegration of the platform(s) and the appearance of flysch basins began in the Late Cretaceous, while the transition from the Cretaceous to the Palaeogene was marked everywhere on the AdCP by a period of emersion. Intense tectonics continued through the Palaeogene, with carbonate deposition on carbonate ramps, while tectonic contraction of the platform area during the Oligocene-Miocene resulted in the uplift of the Dinarides. One of the most distinctive features of the Dinarides is the widespread occurrence of ophiolites generated in subduction processes, first in Dinaridic Tethys and later in the back-arc basin (PAMIĆ et al., 2002). The obducted ophiolites are predominantly peridotite tectonites, enriched in REE typical for ultramafic rocks.

Occurrences and deposits of bauxites can be found at several stratigraphic levels over the entire region of the Croatian Karst Dinarides – from Istria to Dalmatia (ŠINKOVEC & SAKAČ, 1981; SAKAČ et al., 1978; ŠEBEČIĆ et al., 1985; SAKAČ et al., 1984). Some (predominantly of Upper Eocene age from the Outer Dinarides), had large reserves of significant, economy-grade bauxite ore, but these are for the most part totally exhausted. Considering the whole formative period of the AdCP, the Palaeogene was particularly distinctive by a substantial shift of bauxite formation toward the more external zones of the External (Outer) Dinarides (ŠINKOVEC & SAKAČ, 1991). As a result, the majority of deposits formed between the Palaeocene and Upper Eocene, before the final disintegration of the platform that culminated during the Oligocene-Miocene (VLAHOVIĆ et al., 2005). Before that, at the onset of the Tertiary period, Pc bauxites formed extensively over the low-lying, emerged SW part of the AdCP including Istria (Adriatic SW unit), Adriatic islands, and most of Dalmatian hinterland (Dinaridic SW unit) (KORBAR, 2009) occurring almost invariably in the form of small-size, economically often insignificant, ore bodies.

2.2. Field and analytical procedures

2.2.1. Sampling

A total of 50 bauxite samples of Palaeocene age were collected from various sites (deposits and occurrences) in Istria (21), on the North Adriatic islands (12) including Krk, Cres, Rab, Goli and Pag, in Northern Dalmatia (8) and in Central Dalmatia (9). At all locations samples represent the bulk geochemical signa-

ture of bauxites infilling a single regional unconformity (Cretaceous-Palaeogene transition), irrespective of particular horizons within the ore body (e.g. at the contact with the related palaeokarst), possibly with a different geochemical signal related to issues of bauxite autochthony-allochthony or vadose-phreatic depositional-diagenetic environments (D'ARGENIO & MINDSZENTY, 1995; BARDOSSY, 1982). It is presupposed here that multivariate analysis performed on the bulk geochemistry of a number of samples, can pinpoint the most important geochemical processes, by averaging all details down the vertical profile. Detailed investigation at a single site ought to be performed later in order to screen geochemical and mineralogical data with particular reference to processes controlling the geochemical facies of bauxites in a specific part of the lithologic column. It must also be noted in passing, that all investigated bauxites are treated as being of Lower Paleogene (Pc) age, according to the age of the cover rocks, in spite of a possibility that some Istrian bauxites may have formed during more than one emergent stage due to a prolonged hiatus marked by non-deposition (ŠINKOVEC, 1973).

2.2.2. Sample preparation and analysis

Fresh bauxite samples weighing about 3 kg in total were chipped and crushed by hand and finally split into fractions by quartering. Whole-rock samples were subsequently ground in a tungsten carbide pestle mortar mill (Retsch Lab Equipment) to pass through a <0.063 mm sieve to be prepared for the analytical work.

Chemical analysis was performed at the ACME Analytical Laboratories in Vancouver, Canada, using the Lithogeochemical Whole Rock Major and Trace Element analytical method. Total abundances of the major oxides and several minor elements are reported on a 0.2g sample analysed by ICP-emission spectrometry following a Lithium metaborate/tetraborate fusion and dilute nitric acid digestion. Total trace elements were analyzed by ICP-MS. Refractory elements underwent the same decomposition as the major elements (additional 0.2 g sample) while the rest are digested in hot Aqua Regia and analyzed by ICP Mass Spectrometry (0.5 g sample). Bauxite samples were analysed for a total of 32 elements including 10 major element (oxides): SiO_2, Al_2O_3 Fe_2O_3, MgO, CaO, Na_2O, K_2O, TiO_2, P_2O_5 and MnO; and 22 trace elements: As, Ba, Cd, Ce, Co, Cr, Cu, Ga, Hg, La, Mo, Nb, Ni, Pb, Sc, Sr, Th, U, V, Y, Zn and Zr.

Mineralogical analysis was performed by X-ray diffraction (XRD analysis) where the mineral composition of all samples was determined by the PANalytical X'Pert Powder diffractometer. The device is equipped with Ni-filter Cu$K\alpha$ radiation, vertical goniometer with θ/θ geometry and PIXcel detector. Scan conditions were: 45kV and 40 mA, ¼ divergence slit and ½ antiscatter slits, step size 0.02° 2θ, time per step 2s. The sieved samples were then back-loaded on aluminum holders, to ensure random mineral orientation. Powder diffraction data were collected in the range of 5-66° 2Θ. Mineralogical analysis was performed on four samples prepared in the same manner as for geochemical analysis. Only one sample representative of each single group was selected for the purpose. Selection was based on the mean value of

the major-element compositions so that the least value of the Squared Mahalanobis Distance (SMD) for each group (the least distance from the group centroid), was used as a criterion. Mineralogical analysis was obtained by XRD on the bulk samples (IPC-7, KRK-4, DR-11, and IMPC-1). The following mineral compositions were determined: boehmite, haematite, goethite and anatase in samples DR11, IMPC1 and KRK4. Sample IPC7 is different because it contains gibbsite which doesn't appear in other samples. Boehmite is a dominant mineral phase in the 3 samples, while haematite, goethite and anatase appear in minor amounts. Boehmite was determined by the diffractions maximums on d=6.10, 3.16, 2.34 and 1.86 Å. Haematite has its characteristic peaks on d=3.68, 2.69, 2.51 and 1.69 Å. Goethite has diffraction maximums on d=4.16, 2.69 and 2.45 Å. Anatase was identified by peaks d=3.51, 2.37 and 1.66 Å. Gibbsite appears only in sample IPC7 and was determined by strong reflection peaks on d=4.84, 4.37 and 3.31 Å.

3. STATISTICAL CONSIDERATIONS

3.1. The data

A set of 32 elements including 10 major and 22 trace elements was selected as predictor variables in building the original discriminant model. Summary statistics for the whole dataset prior to the multivariate statistical procedure are displayed in Table 1 (minimum, maximum, median, mean, standard deviation and skewness). Since most of the variables are characterized by non-normal, positively skewed, frequency distributions (except Al_2O_3 and TiO_2, Ga, Nb, Th and Zr which are negatively skewed), appropriate transformations were found necessary to acquire a more symmetric distribution. As a general rule, most geochemical data do not follow normal (neither lognormal) distribution (e.g. MATSCHULLAT et al. 2000; REIMANN & FILZMOSER, 2000; REIMANN et al. 2005); a problem arising from complex non-linear dynamics, feedbacks and thresholds within a natural system characterized by the particular suite of variables (e.g. HUGGET 1998; PHILLIPS, 1999). Univariate distributions of the input data were examined by the Shapiro-Wilks W test of normality (added to Table 1 as p-values before and after normalization). Conventional normalization procedure using log-transformations was subsequently applied where necessary to stabilize the variance of the original data. This process included all the major elements except P_2O_5, and a greater part of the trace elements exclusive of Ga, La, Nb, Sc, Th and Zr which are normally distributed (all marked by the asterisk). According to the applied test, 17 more variables attained normal distribution after normalization (SiO_2, Fe_2O_3, MgO, CaO, As, Ba, Cd, Ce, Co, Cu, Hg, Mo, Pb, Sr, V, Y and Zn (p>0.05, marked by double asterisk)). However, where the normalization procedure failed, having produced an even greater skew with respect to the original distribution (such as with Al_2O_3 and Na_2O), the data were rather left untransformed. As with all multivariate statistical procedures, yet another assumption had to be made before DFA can be successfully utilized in research – that of sufficient sample size supplying enough information upon which to found analysis. Based on the variety of general recommendations considering the importance

of sample size and sample-to-size ratio reviewed in a number of works (e.g. ARRINDEL & van der ENDE, 1985) 50 observations was deemed sufficient but major and trace elements were analyzed as separate data matrices.

3.2. Building a discriminant function model (DFM)

Multiple (multi-group) discrimination analysis (MDA) is a statistical technique that is particularly useful when applied to distinguish between several pre-defined groups based on a great number of observations. Its purpose, defined in a statistical sense, is to maximize the between-group variance in comparison to the variance within each group (e.g. DILLON & GOLDSTEIN, 1984). In the process, a hypothesis is tested that all observed groups have the same multivariate mean against the alternative that at least one multivariate mean is different (ROCK, 1988). Provided that alternative hypothesis is accepted (which does not mean that each pair of groups must necessarily be plainly separated and distinct), the original set of data is then recalculated by MDA into a number of discriminant scores, allocating each object or group (the latter represented by its mean), along one or more lines – linear discriminant functions (e.g. KRUMBEIN & GREYBILL, 1965; DOORNKAMP & KING, 1971; DAVIS, 1986). In this way the multivariate problem simply collapses into a fewer-dimension solution, one less than the number of groups (K-1), or equal to the number of variables (p), whichever is the smaller.

Here, discriminant analysis from the statistical software package of STATISTICA, Release 7.1 (StatSoft, Inc., 2006) was used to investigate chemical differences between the four groups of bauxites separated previously by independent criteria such as their geographical position and palaeotectonic settings within the AdCP as a major geotectonic unit. The groups containing 50 samples were determined as Early Palaeogene (Palaeocene) bauxites and sampled from different quarters of the AdCP, namely Istria (IST), North-Adriatic Islands (NAI), North Dalmatia (NDA), and Central Dalmatia (CDA), roughly following the position of the formerly established tectonostratigraphic units (KORBAR, 2009). In order to achieve the best separation between groups and explain the geological causes underlying the structure of input data, two discriminant models were constructed based on the two sets of predictor variables, namely the bulk concentrations of major (10) and trace elements (22).

4. RESULTS AND DISCUSSION

The results of the MDA are briefly summarized in the joint table (Tab. 2) comprising both research models containing major and trace elements. The overall significance of their discrimination is tested by the appropriate multivariate tests (Tab. 3) showing the extremely low associated probabilities (p<0.000) in both cases, which is required to safely proceed with computing discriminant functions (DFs). Since the same number of groups (K=4) is studied in both models, the between-group variation is completely explained by the three DFs (K-1). Table 2 reveals that in both models, DF1 explains

Table 1: Descriptive statistics.

Element	Min	Mean	Med	Max	StDev	Skew	S–W(p)	S–W(p₁)
SiO_2 (%)	1.02	3.914	3.415	9.10	2.059	0.825	0.004	**0.560
Al_2O_3 (%)	34.50	50.114	50.415	58.58	5.308	-0.890	0.021	–
Fe_2O_3 (%)	14.76	26.114	25.955	45.96	5.294	0.993	0.027	**0.750
MgO (%)	0.06	0.137	0.11	0.49	0.077	2.388	0	**0.070
CaO (%)	0.04	0.126	0.115	0.64	0.094	3.525	0	**0.116
Na_2O (%)	0.005	0.02	0.01	0.33	0.046	6.664	0	–
K_2O (%)	0.005	0.046	0.03	0.20	0.047	1.761	0	0.012
TiO_2 (%)	1.60	2.889	2.955	3.88	0.493	−0.699	0.030	0.030
P_2O_5 (%)	0.005	0.054	0.053	0.113	0.025	0.046	*0.608	–
MnO (%)	0.02	0.079	0.05	0.46	0.083	3.256	0	0.013
As (mg/kg)	1.7	39.198	36.15	154.9	32.304	1.844	0	**0.132
Ba (mg/kg)	6.0	26.280	24.0	73.0	13.028	1.749	0	**0.117
Cd (mg/kg)	0.1	2.03	1.2	11.0	2.438	2.250	0	**0.567
Ce (mg/kg)	64.6	233.218	193.8	645.3	130.050	1.321	0	**0.825
Co (mg/kg)	14.2	41.33	38.2	91.9	16.866	1.070	0.004	**0.985
Cr (mg/kg)	362.76	713.07	578.37	1423.62	309.056	0.835	0	0.003
Cu (mg/kg)	21.9	102.672	82.3	250.5	60.749	1.087	0	**0.503
Ga (mg/kg)	33.6	53.024	53.55	65.1	7.309	-0.662	*0.104	–
Hg (mg/kg)	0.03	0.314	0.225	1.02	0.256	1.135	0	**0.189
La (mg/kg)	40.7	99.106	93.8	179.3	31.209	0.386	*0.141	–
Mo (mg/kg)	0.9	9.89	7.55	33.0	7.961	1.125	0	**0.237
Nb (mg/kg)	30.7	57.278	59.4	75.4	9.154	−0.774	*0.057	–
Ni (mg/kg)	88.0	256.76	224.5	1092.0	178.974	3.094	0	0.003
Pb (mg/kg)	44.2	103.018	97.6	196.6	33.985	0.828	0.030	**0.842
Sc (mg/kg)	35.0	57.5	54.0	91.0	13.239	0.624	*0.096	–
Sr (mg/kg)	27.6	81.728	74.7	220.4	36.582	1.489	0	**0.240
Th (mg/kg)	28.5	45.704	45.25	60.7	6.351	−0.224	*0.496	–
U (mg/kg)	4.6	9.076	8.7	26.9	3.565	2.834	0	0.025
V (mg/kg)	286.0	622.24	539.0	1876.0	312.099	1.938	0	**0.064
Y (mg/kg)	31.4	85.392	69.7	255.9	45.305	2.163	0	**0.072
Zn (mg/kg)	12.0	125.180	90.0	422.0	92.700	1.090	0	**0.340
Zr (mg/kg)	312.3	530.06	532.55	721.2	81.161	-0.611	*0.116	–

the largest portion of the total variability hidden within the original main- and trace elements data spread, amounting to almost 80% for the latter. Note, however, that in the trace-element DFM the third function (DF3) exhibits a low contribution to the total variance, which can be seen both by the tested significance (p=0.146) and low eigenvalues (Tab. 2), meaning that only the first two DFs are sufficient to separate the four bauxite groups based on their trace element content.

4.1. Functional models
(Labeling discriminant space)

Labelling DFs is an essential part of the analysis since it offers a geologically meaningful interpretation to the whole discrimination scheme. Through this process the hidden mathematical

Table 2: Tests of residual roots (discriminant functions) for both DFMs.

DF	Eigen value	Eigen (%)	Canon. R	Wilks ▶▶	chi²	df	p-level
			Major-element DFM				
1	2.385	56.93	0.839	0.082	104.9	30	0.000
2	1.067	25.46	0.718	0.278	53.7	18	0.000
3	0.737	17.61	0.651	0.576	23.2	8	0.003
			Trace-element DFM				
1	24.283	79.42	0.980	0.003	208.6	66	0.000
2	5.199	17.00	0.916	0.077	92.3	42	0.000
3	1.094	3.58	0.723	0.477	26.6	20	0.146

Table 3: Multivariate test for overall significance of discrimination.

	Major-element DFM	Trace-element DFM
No. of variables	10	22
Wilks lambda	0.082	0.003
Approximate F ratio	4.888	6.818
Degrees of freedom	[30; 109]	[66; 75]
p-level	p < 0.000	p < 0.000

structure underlying the raw geochemical observations can be easily exposed to the observer. Discriminant loadings (simple correlations of variables with respective DFs), or structure coefficients, are particularly useful in clarifying the individual contribution of each descriptor variable (major and trace elements), to the overall discrimination. In this sense the variables with small discriminant loadings which contribute little to the explanatory power of DFs in both DFM are seen as irrelevant and can be eliminated from further consideration. This is easily seen on the variable diagrams that provide the quickest and most informative insight into the structure of discriminant space, suggesting also which subset of variables (descriptors) most clearly separates the *a priori* defined groups (Figs. 2a, 3a and 5a). Obviously, elements clustered more or less tightly around the intersection of discriminant axes such as SiO_2, Fe_2O_3 and Na_2O in major-element DFM, and the majority of elements in trace-element DFM excluding Cr, V, As, Ga and some others, do not form the best subset required for meaningful interpretation of DFs in terms of geological processes.

Association among descriptor variables and related groups is best represented geometrically, viewing the DFs as orthogonal axes intersecting in the reduced discriminant space. However, it is not possible to compare the variable and group scatterplots directly, since different scales are used in each case. The scatterplots of variable loadings (Figs. 2a, 3a and 5a) display discriminant axes as normalized vectors, while the scatterplots of canonical means (group centroids), and individual objects (samples), display discriminant score vectors (Figs. 2b, 3b and 5b). Thus, reciprocity between the variables and groups should always be considered using their shared position along the appropriate axis.

4.1.1. Major-element model

In the major-element model, all three DFs are highly significant with DF1 explaining considerably over half of the total variation (57%) between the groups (Tab. 2). As seen from the scatterplot of variable loadings (Fig. 2a), DF1 is slightly bipolar, primarily separating the Istrian group of Palaeocene bauxites (IST), from both the Central Dalmatian (CDA) and North Dalmatian (NDA) groups, while bauxites from the North-Adriatic islands (NAI) remain largely undistinguished (Fig. 2b). The rationale for this separation is founded in the negative association between the K_2O–TiO_2 variable set on the one side and P_2O_5 on the other. Geochemically, it can be understood as IST bauxites being enriched in K_2O–TiO_2 and depleted in P_2O_5 with regards to NDA and CDA bauxites, and vice versa. Although the overlap is considerable between
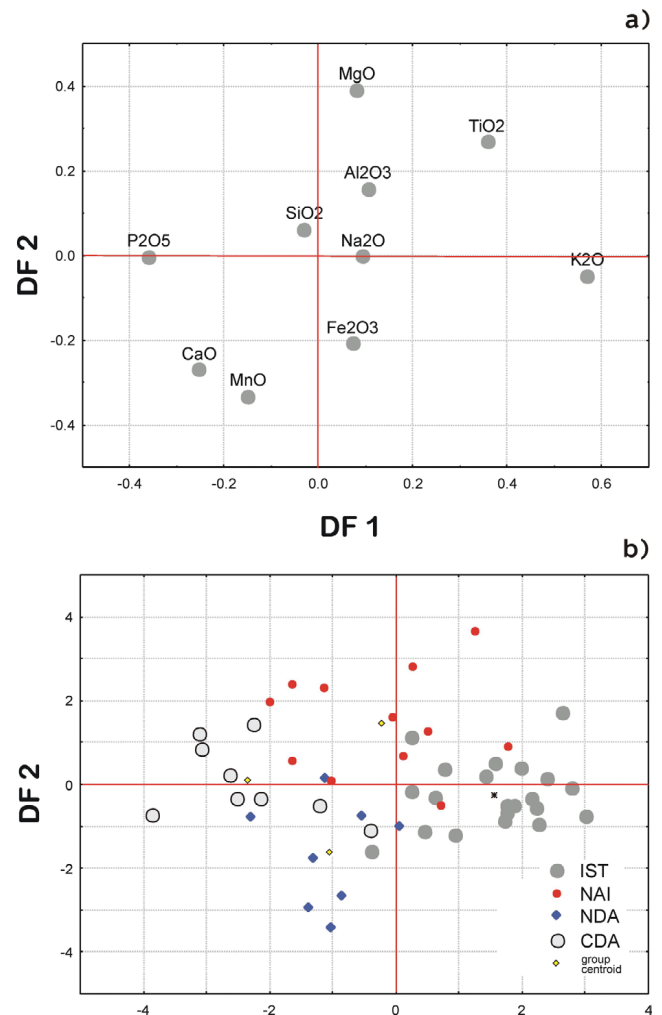
Figure 2: Comparison between variables and groups in the major-element DFM: scatterplots of (a) variable loadings and (b) individual objects (samples) in reduced discriminant space of the first two discriminant functions (DF1-DF2).

all groups, a distinct change in content of respective elements can be easily detected if groups are placed in the appropriate palaeogeographic/palaeotectonic setting over the investigated part of AdCP. Four bauxite groups are regularly scattered in the IST-NAI-NDA-CDA succession following the NW-SE strike of the Upper Cretaceous-Paleogene boundary (except in Istria where hanging-wall sediments were completely removed). A small but regular decrease in the K_2O–TiO_2 association is easily observable from Istria towards Central Dalmatia (from right to left on the sample-centroid scatterplot, Fig. 2b). Thus, the geological interpretation of DF1 can be established on the "enrichment-depletion" relationship of K_2O–TiO_2/P_2O_5 variable opposites with reference to their specific palaeotectonic setting within the AdCP. It must be noted, however, that the central position of the NAI bauxites, close to the main centroid and overlapping both IST and CDA bauxites, indicates the average major-element composition of a "transitory" group. A general decrease in the K_2O–TiO_2 content in Palaeocene (Pc) bauxites in a NW-SE direction, from Istria to Dalmatia, can be associated with differing palaeographical conditions at various parts of the

AdCP since the Cretaceous-Paleogene transition (VLAHOVIĆ et al., 2005; KORBAR, 2009). Geodynamic evolution of the External Dinarides in post-Mesozoic times may have caused a prolonged exposure of primary bauxites, accounting for recurrent contamination by airborne (aeolian dust or volcanic ash), or terrigenous (fluvial) sedimentary material. Due to the extended hiatus lasting in parts of Istria from the Early Cretaceous (shallow-water carbonates) to the Early Eocene (foraminiferal limestones) (KORBAR, 2009, and references therein) Istrian bauxites (IST) may have been graded and degraded repeatedly due to the input of new material and changing environmental conditions (e.g. discontinued leaching as a result of changing climate or drainage conditions), and thus never deprived completely of clayey (particularly illitic) material. This reworking is advocated by the mineralogical (XRD) analysis showing that only the bauxites from the SE part of the Dinaridic SW unit (CDA) contain gibbsite (hydrargillite), which is the constituent part of the primary bauxites, while other investigated groups (IST+NAI+NDA) are boehmitic (Fig. 4). Since the primary (gibbsitic) karst bauxites are rarely preserved in the Mediterranean area (HOSE, 1986), the dehydration of gibbsite into boehmite as an end-product of intensive aluminosilicate weathering in a subtropical environment (palaeosols and recent soils of tropical and subtropical areas) with potentially high leaching rates (HERRMANN et al., 2007; D'ARGENIO & MINDSZENTY, 1995; KLEBER et al., 2007) must have been a common process in the most parts of the AdCP during the Cretaceous-Palaeogene transition. However, Pc bauxites from the Imotski area (CDA) are predominantly gibbsitic (Fig. 4; Tab. 4) indicating prevalently hydrous conditions (intense leaching due to intense rainfall and rapid drainage, CHORLEY et al., 1985) during most of the relatively short emersion stage. Mineralogical analysis also demonstrates the absence of anatase as a dominant TiO_2 polymorph usually present in other groups. The low content of TiO_2 is characteristic of the CDA group while being abundant in the IST and NAI (up to 3.88 % in KRK-2 sample) together with K_2O (Fig 2a, b), meaning that at least a portion of the TiO_2 component must have been enriched by reworking primary bauxites after being formed as fine-grained anatase as a result of weathering of the titanium-bearing silicates, similar to recent regoliths (FORCE, 1991). Conversely, most of the P_2O_5 can be co-precipitated with Fe-Mn oxy-hydroxides (goethite) under oxidative conditions. It is well known that phosphate adsorption by goethite and other Fe oxides strongly influence its concentrations in soils and aquatic environments (TORRENT et al., 1992). This interaction must also have been
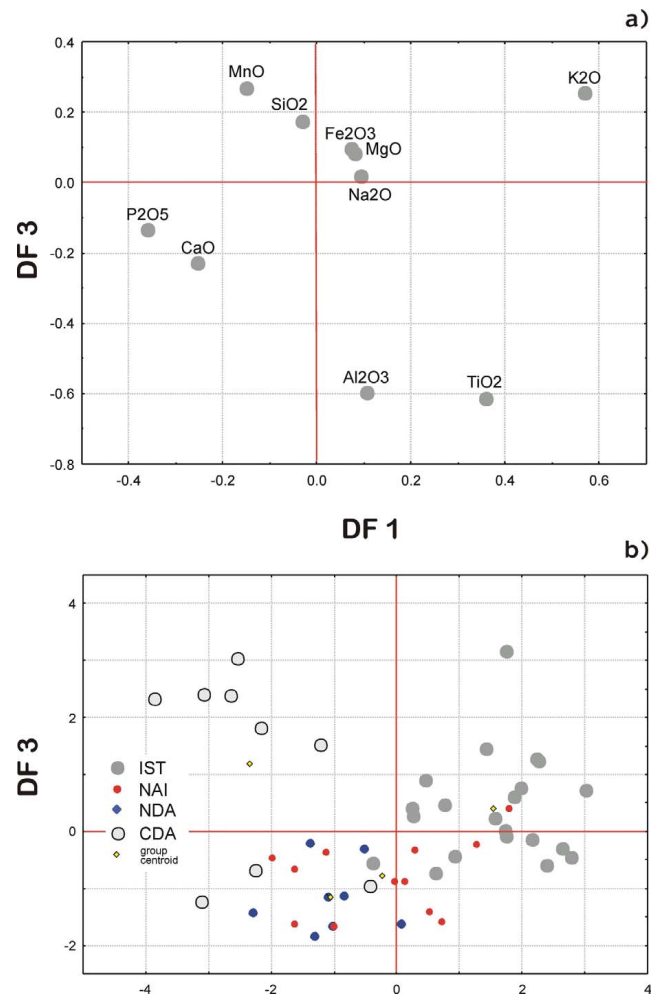

Figure 3: Comparison between variables and groups in the major-element DFM: scatterplots of (c) variable loadings and (d) individual objects (samples) in reduced discriminant space of the first and third discriminant functions (DF1-DF3).

important in controlling phosphate in the bauxite-forming palaeoenvironment. Although DF1 is generally neutral with regards to Fe_2O_3, the P_2O_5 content is loosely associated with MnO at the negative pole of the function, indicating the possible scavenging role of Mn-oxyhydroxides as a proxy channel for phosphorus accumulation in CDA bauxites. However, an even closer association of the CaO component with P_2O_5 points to apatite as the main phosphorus phase (Fig. 2a). Apatite is a widespread accessory phase in the magmatic sequence of ophiolite complexes and is widely documented in literature describing the Ni-Cr-rich ophiolite-derived laterites of Northern Greece (e.g. ECONOMOU-ELIOPOULOS, 2003). Not suprisingly, perhaps, the lowest P_2O_5 concentrations are observed in IST bauxites at the westernmost part of the AdCP (commonly below 0.01%; 0.04% in average) far from the Dinaridic Ophiolite Zone. Alternatively, high values can be found in all groups (up to 0.11% in NDA or 0.10% in NAI) indicating that removal of P_2O_5, more than enrichment was typical for the bauxite-forming environment, being most effective over the Istrian Peninsula.

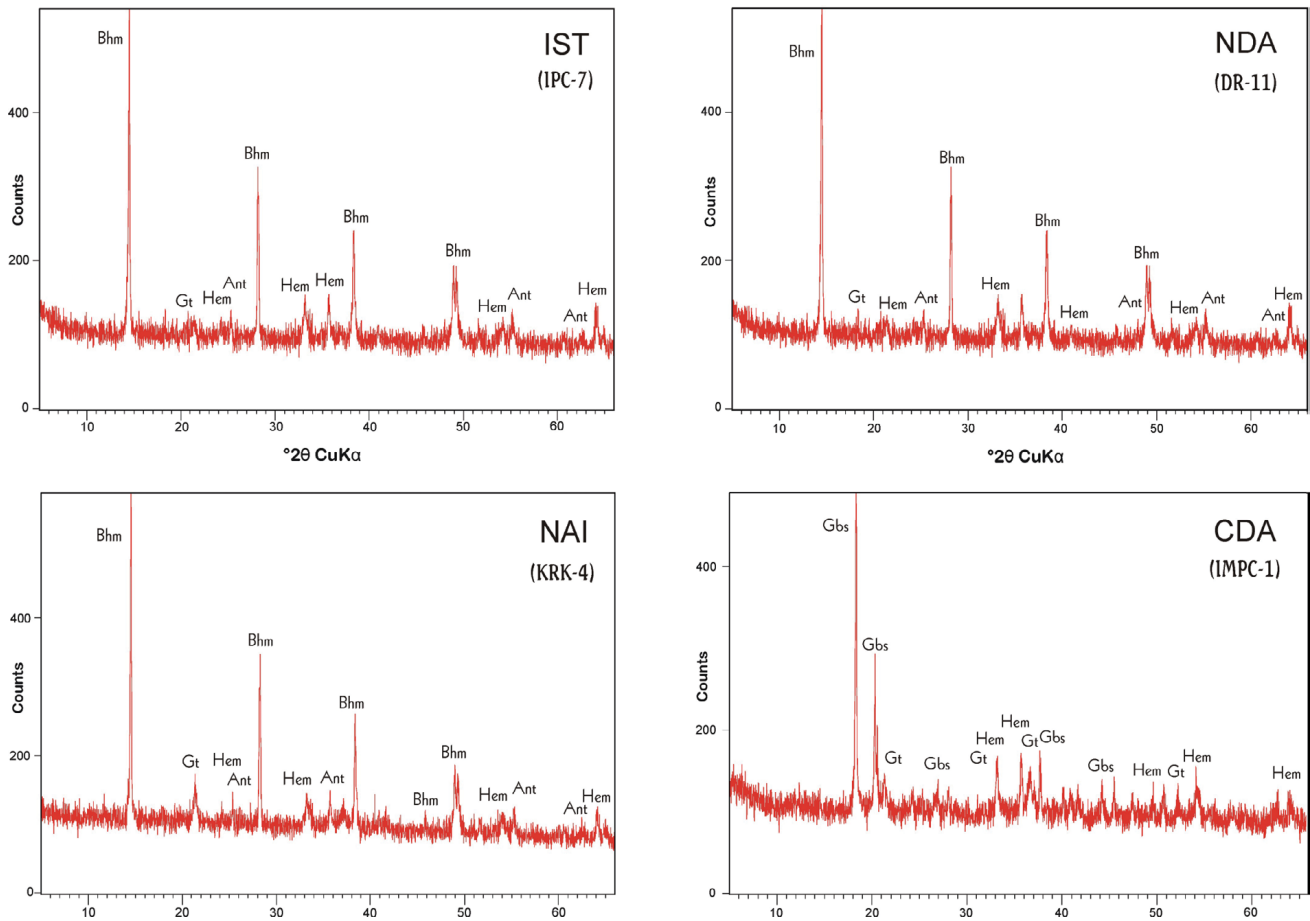It is evident from above that DF1 can be functionally explained from the perspective of changing environmental

Table 4: Qualitative mineral composition of the main components in Pc bauxites.

Sample	Mineral content
DR-11	boehmite, haematite, goethite, anatase
IMPC-1	gibbsite, haematite, goethite
IPC-7	boehmite, haematite, goethite, anatase
KRK-4	boehmite, haematite, goethite, anatase

Figure 4: X-ray diffractograms of four Early Palaeogene bauxite samples from the Croatian part of the AdCP.

(palaeogeographical) conditions prevailing during the AdCP Cretaceous-Paleogene emergent phase which resulted in a particular "enrichment-depletion" major-element signature.

Although statistically highly significant in the major-element model, the other two discriminant functions DF2 and DF3 explain a smaller fraction of the total variation (25.5 and 17.6 %, respectively), adding some new insight into the geochemical interpretation of the all-important DF1. Clarification of DF2 revolves primarily about separating the two "inner" groups among the palaeogeographically established IST→CDA sequence within the AdCP. Although not easily observed from the group scatterplot (Fig. 2b) it is essential that the "end groups" in this succession (IST vs. CDA) do not lose their members to each other (Tab. 5). However, DF2 separates between NAI and NDA with extremely high efficiency in that only one in 20 bauxite samples is lost to other group (NDA to NAI). Discrimination between NDA and NAI is based on the polarity relationship between the MnO–$(CaO$–$Fe_2O_3)/MgO$ major-element suite, which is possibly a reflection of palaeodynamic and palaeoclimatic conditions prevailing in the central portion of the investigated bauxite-bearing Croatian high karst area (External Dinarides) during the Cretaceous-Palaeogene transition. The recent hinterland part of the AdCP (NDA bauxites), can be seen as an ancient repository for the hydrothermally derived marine manganese input from the pelagic realms caused primarily by tectonic/eustatic changes (CORBIN et al., 2000, and references therein). In this context the higher manganese content would correspond to a transgressive maximum, whereas the lower content to a regressive maximum. According to CHESTER (1990), almost 90% of continental Mn is trapped within coastal and estuarine environments, accounting for periodic ingress of marine waters into terrestrial and lacustrine systems of very low plate-interior relief (D'ARGENIO & MINDSZENTY, 1995). This would explain the elevated content of MnO (with Fe_2O_3 and CaO) in NDA bauxites having occurred immediately before or during the final subsidence of emergent platform areas and subsequent diagenesis of buried bauxite (Fe-Mn oxy-hydroxides precipitated in oxygen-rich waters). In contrast, the increased content of MgO in NAI bauxites may indicate an indurate subaerial setting, characterized by an interim shift to more arid conditions, with limited percolation of meteoric waters in primary bauxites, which results in inefficient removal of Mg ions and formation of Mg-rich clays (KETZER et al., 2003), indicated by an MgO–$(TiO_2$–$Al_2O_3)$, as opposed to a MnO–$(CaO$–$Fe_2O_3)$ major-element signature, although other scenarios for relative Mg-enrichment are possible.

The third discriminant function DF3 (Figs. 3a, b) is essentially monopolar, and it highlights a specific major-ele-

Table 5: Classification matrix.

OBSERVED GROUPS	PREDICTED GROUPS											
	Major-element DFM						Trace-element DFM					
	IST	NAI	NDA	CDA	Total	% correct	IST	NAI	NDA	CDA	Total	% correct
IST	19	1	1	0	21	90.48	21	0	0	0	21	100.0
NAI	2	10	0	0	12	83.33	0	12	0	0	12	100.0
NDA	0	1	7	0	8	87.50	0	0	8	0	8	100.0
CDA	0	1	1	7	9	77.78	0	0	0	9	9	100.0
Total	**21**	**13**	**9**	**7**	**50**	**86.00**	**21**	**12**	**8**	**9**	**50**	**100.0**

ment pattern which is largely concerned with separation of aluminum (Al_2O_3) and titanium oxides (TiO_2), from the suite of elements including the clayey component from the rest (K_2O–SiO_2–MgO–Na_2O). Accordingly, DF3 separates basically on the ground of the clay content in bauxites, with variations (MnO, Fe_2O_3), explained earlier as the degree of leaching efficiency and hydrolysis, and relates most particularly to the CDA bauxites. It is thus a supplement to DF1, but reveals a distinct gap within the single group dividing most of its members from the primary IST-NAI-NDA-CDA sequence. This separation refers to specific conditions in a part of CDA bauxitiferous environment distinguished by sluggish removal of leachates, probably due to low amounts of free percolation in waterlogged situations and the occurrence of montmorillonite, illite and chlorite as the resulting clay products (CHORLEY et al., 1985). It must be noted that DF3 also reveals some intrinsic heterogeneity within the IST group which probably can be ascribed to changing palaeogeographic and palaeoclimatic changes during the long hiatus, having affected the northernmost portion of AdCP. This refers most to IPC-14 where the bauxites, after being reworked, have never been completely leached out (K_2O and other clay constituents) but must have undergone conditions of impeded drainage due to periodic rising of the water table (swamps).

4.1.2. Trace-element model

Unlike the major-element DFM only two DFs are statistically significant in the trace-element DFM (Tab. 2), of which DF1 accounts for almost 80% of the variation between the groups. This model is a clear-cut example of how individual objects can be unambiguously assigned into their *a priori* defined groups (Figs. 5a, b). The classification efficiency is 100%, implying total separation between the four investigated groups of bauxites (Tab. 5). This is strongly opposed to the major-element DFM where group division is somewhat blurred, in spite of the same criterion applied in discrimination. The group assignment details based on the Squared Mahalanobis Distance (SMD), also show that distances between the groups are considerably larger than in the major-element DFM (Tab. 6), with a difference that NDA is placed further away from IST (IST/NDA = 120.72), than CDA (IST/CDA = 111.31), modifying the mathematically defined geochemical-(palaeo)geographical distance pattern found between the groups in the major-element DFM. Com-
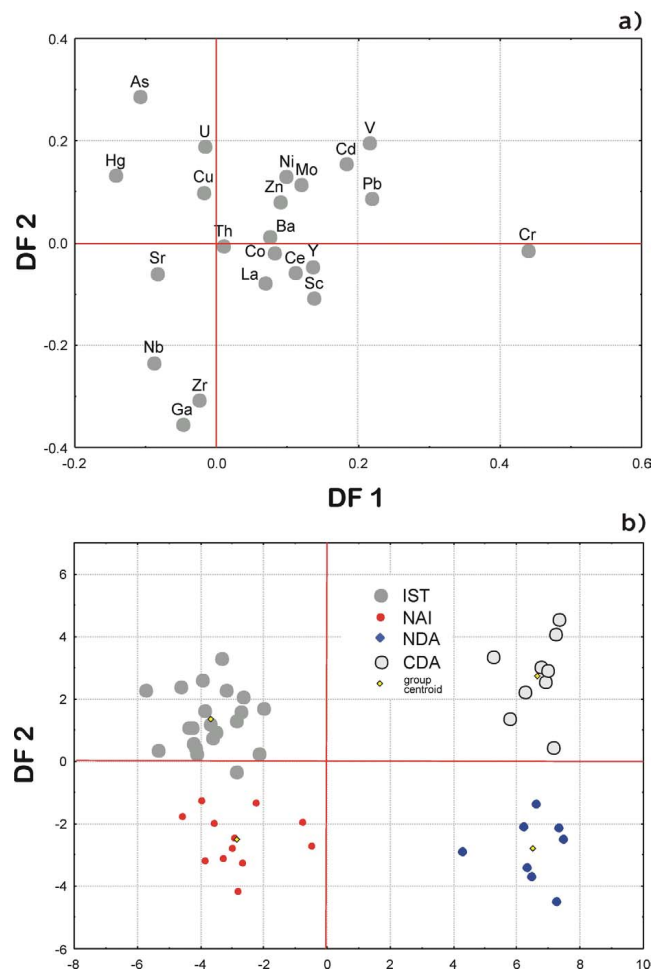

Figure 5: Comparison between variables and groups in the trace-element DFM: scatterplots of variable loadings (a) and individual objects (samples) (b) in reduced discriminant space of the first two discriminant functions (DF1-DF2).

Table 6: Squared Mahalanobis Distance (SMD).

GROUP	Major-element DFM				Trace-element DFM			
	IST	NAI	NDA	CDA	IST	NAI	NDA	CDA
IST	0.00				0.00			
NAI	7.54	0.00			18.64	0.00		
NDA	11.13	10.54	0.00		120.72	94.14	0.00	
CDA	15.94	10.31	10.11	0.00	111.31	117.54	35.83	0.00

plete/incomplete separation between groups based on the major-element/trace-element signature was observed earlier in similar investigations (PEH & HALAMIĆ, 2010), and can be explained on the grounds that major elements enter various processes active during the sedimentary cycle (from weathering to burial and diagenesis), while accumulation or depletion of trace elements usually narrows the scope of research to some particular segment of the cycle.

DF1 is essentially a monopolar function and it can be interpreted geochemically as reflecting a particular position of Cr against a number of trace elements with low discriminatory potential, clustered around the main centroid. Chromium is typically enriched in ultramafic and mafic rocks together with Ni although the latter is not so prominent in the analyzed bauxites (Fig. 5a). Elevated values of Cr in bauxites can be indicative of ophiolitic complexes containing ultramafics and related rocks as a parent material, particularly given its very low mobility even in strongly-weathered environments, but especially under moderately oxidizing and reducing conditions and near-neutral pH values (De VOS et al., 2006). Together with other trace elements such as Ti and Zr in particular, which are considered immobile during weathering and hydrothermal alteration processes (MACLEAN & BARRET, 1993), the ratios Cr forms in bauxites do not differ greatly from those in parent rocks (VALETON et al., 1987) and thus can be applied in bivariate or ternary diagrams for determination of the parent material. It is clear from the diagrams (Figs. 5a, b) that a clear-cut split between the group pairs caused by Cr-enrichment in NDA and CDA bauxites from the central and SE parts of the investigated AdCP (High Karst Dinaridic unit), must suggest an extraneous source of chromium – most probably the Dinaridic ophiolite belt with large ultramafic massif and radiolarite formation (PAMIĆ et al., 2002) at the AdCP NE border as its host rocks. In contrast, IST and NAI bauxite groups of the Istrian Karst Adriatic unit and northern part of the High Karst Dinaridic unit, respectively, contain below-average Cr content. Typically, Cr-content amounts to 1232 mg/kg in NDA or even up to 1424 mg/kg in CDA with mean values of 1053 mg/kg and 1142 mg/kg, respectively. This enrichment is considerably higher than that for the majority of Mediterranean karst bauxites of various stratigraphic positions including the Upper Palaeogene (Eocene) bauxites from the Obrovac area (CALAGARI & ABEDINI, 2007). Conversely, IST bauxites contain only 489 mg/kg of Cr on average while NAI bauxites are slightly more enriched; 556 mg/kg indicating a completely different (felsic) lithological provenance. Indicatively, modern soils from North and Central Dalmatia are highly enriched in chromium (up to 444 mg/kg, Obrovac area), being most possibly contaminated by the nearby bauxite deposits, albeit mostly of Eocene age, abounding in the area (HALAMIĆ & MIKO, 2009). Determination of the possible precursor rock type can be easily deduced from the ternary diagram comparing the Cr, Zr and Ga concentration values of Palaeocene bauxites formed on the AdCP (Fig. 6). If compared to corresponding trace-element DFM scatterplots (Figs. 5a, b), a striking shift of NDA and CDA groups

to the mafic and ultramafic field is obvious drawing these bauxites near to those in bordering Bosnia and Herzegovina, or even farther east in Greece (ÖZLÜ, 2004; CALAGARI & ABEDINI, 2007, and references therein).

Apart from chromium, DF1 is characterized by small-scale variations in the content of other trace elements and only their relative position with respect to the main centroid indicates slightly elevated concentrations of V, Cd and Pb (as well as slightly decreased concentration of As, Hg and others) in CDA and NDA groups with respect to IST and NAI groups, and vice versa.

The second discriminant function DF2 is slightly bipolar and contains considerably lower explanatory potential with respect to DF1 (only 17%). It is marked by a negative association between As and the suite of trace elements including Ga, Zr and possibly Nb. However, this relationship calls for caution due to commonly weak variable loadings which renders its geological interpretation rather speculative. An inverse relationship between the two trace-element assemblages could be interpreted as representing differing conditions relating to provenance, weathering and deposition during the early stages of bauxite formation, which strongly affect their chemical behaviour. Since genesis of primary bauxites in many facets resembles the formation of red claystone and terra rossa soils after the subsequent pedogenesis (MERINO & BANERJEE, 2008), it is possible to treat their trace element geochemistry in a similar way as in palaeosols, whether related to weathering intensity, evaluation of leaching, or provenance (SHELDON, 2009). Elements of interest in this context are undoubtedly Zr and Nb which are characteristically relatively immobile during
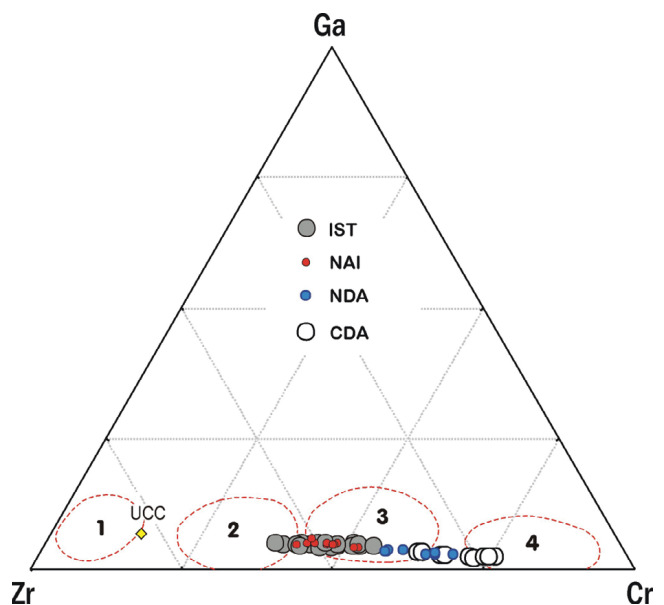

Figure 6: Ternary diagram for Zr, Cr and Ga concentrations in the samples of the four investigated groups of Early Palaeogene bauxites in Croatia; the numbered circles represent the area of influence of felsic (1), intermediate (2), mafic (3) and ultramafic (4) rocks indicated as probable parent material in genesis of the Mediterranean karst bauxites (after ÖZLÜ, 1983); UCC = average Zr-Cr-Ga content in the upper continental crust (after TAYLOR & MCLENNAN, 1985).

weathering of source rocks and bauxite genesis, including Ga which is typically related to Al and processes of intense leaching, linked with supergene (surface or near-surface) environment under tropical and subtropical climates (HIERONYMUS et al., 2001). As DF2 clearly discriminates between the NDA-NAI group pair set apart by a prominent Ga-Zr-Nb association, and a CDA-IST pair characterized by As (Figs. 5a, b), this relationship can possibly highlight the redox conditions controlling the trace-element enrichment-depletion in the bauxite-bearing palaeo-environment. Arsenic accumulation in subaerially formed sedimentary rocks is most often recognized through the process of sorption on Fe oxy-hydroxides, which are precipitated in the form of ooids (goethite) slowly formed under mainly oxic conditions (BANNING & RÜDE, 2010). However, lacking precise XRD analysis, the origin of As is ambivalent in spite of possible significant As-Fe correlation since a variety of processes in the reduced environment may induce co-precipitation of As with Fe sulfides. It is widely believed that sulfidogenesis via microbial SO_4^{-2} reduction can slow down As mobility in reducing subsurface environments (BURTON et al., 2011). Thus, at least a portion of the As accumulated particularly in Istrian bauxites can derive its origin due to precipitation of Fe-sulfide minerals such as pyrite. The presence of sedimentary pyrite in bauxites from Minjera (Istria) (ŠINKOVEC et al., 1994) strongly advocates this possibility. Alternatively, As hosted in CDA bauxites indicates a different origin, since sulfides generally do not function as an important sink for lithophile elements such as Cr (HUERTA-DIAZ AND MORSE, 1992) which abound in CDA bauxites. Most probably, it is present via the Fe-oxyhydroxides (haematite, goethite) derived from the Dinaridic ophiolite complex for which As enrichment is well-documented (e.g. in radiolarian cherts, PEH & HALAMIĆ, 2010).

Conversely, Nb, Zr, and Ga in particular, would indicate hydrous conditions where bases were effectively leached in primary bauxites. That Ga is strongly associated with Al in this process can be easily deduced by the trace- and major-element DFM comparison (Fig. 3a vs. Fig. 5a) which both separate the Al-Ga higher-content NAI and NDA from lower-content IST and CDA groups. However, an obvious mismatch between the diagrams caused by better separation performed by the trace-element DFM may indicate that Al and Ga (including Zr and Nb) do not necessarily follow the same paths controlled by the physico-chemical conditions of the bauxite-bearing environment in all parts of the AdCP. It usually calls for reworking the primary (gibbsitic) bauxites since the tight association between Al and Ga may be disturbed, or even reversed, if gibbsite previously formed by laterization (bauxitization) is later dissolved due to the aforementioned environmental changes. Ga, which is more soluble, tends to be leached out, while Al migrates downward and precipitates again as gibbsite (HIERONYMUS et al., 2009). This was the probable scenario for distinctive absence of Ga (Nb, Zr) in IST and CDA bauxites, although Al is enriched only in rare samples of these groups (in the form of gibbsite in CDA or boehmite in IST bauxites).

5. CONCLUDING REMARKS

Two DFMs were built in this study in order to distinguish geochemically between the four groups of Pc bauxites sampled from the various corners of the Croatian part of the AdCP. The bauxites, having derived from the same regional unconformity, were assumed to have undergone generally similar conditions of formation with regards to global (eustasy and climate), and regional (volcanism and tectonics) controls during the subaerial exposure of the platform. However, the local portions of emergent palaeoenvironment may have easily experienced a slightly different recombination of controlling factors causing variations in depositional and diagenetic facies (most particularly with regards to the amount of free percolation in the weathering mass), and necessarily variable resulting geochemical signature. High performance of separation between the *a priori* defined groups of bauxites achieved by MDA, especially consulting the trace-element DFM, demonstrated a high degree of efficacy in characterizing specific environmental conditions that lead to formation and emplacement of bauxites onto the carbonate platform.

Important results of MDA analysis can be briefly summarized as follows:

– Almost complete separation between the four groups of Pc bauxites from various parts of AdCP (from Istria to the Central Dalmatia) is attained by MDA using the geochemical major- and trace-element data array.

– The major-element DFM demonstrates a lower degree of separation between groups (86 %) with respect to the trace-element DFM owing to the fact that major elements participate in a variety of processes during the sedimentary cycle resulting in the necessary overlap in the a priori naturally defined groups. Typically, the best discrimination between the groups is achieved on DF1, extracting more than a half of the total variability (57 %) via the bipolar K_2O/P_2O_5 "enrichment-depletion" relationship. This pattern can be identified as signaling the multiple reworking of proto-bauxitic material in changing environmental conditions prevailing during the AdCP Cretaceous-Palaeogene emergent phase. Spatially, it is manifested in regular geographical IST-NAI-NDA-CDA succession showing gradual K_2O decrease (P_2O_5 increase) in a SE direction. The functions DF2 and DF3 are of minor importance expounding tectonic/eustatic controls over periodic ingress of marine waters onto the carbonate mainland (MnO, NDA) or long-lasting subaerial exposure (MgO; NAI), and overall degree of maturity characterized by the presence/absence of clay material (enriched Al_2O_3 and TiO_2 components in majority of groups except for some CDA and IST samples), respectively.

– Trace-element DFM is more suitable for both discriminating and identifying purposes since the classification efficiency of the established predictive model is the highest possible (100%). Discrimination is unequivocally based on Cr content which separates the CDA-NDA (Cr-enriched) from the NAI-IST group pair, accounting for almost 80% of the explanation potential of DF1. This most

probably refers to the provenance issues relating the source material of CDA-NDA bauxites to the mafic precursor rocks from the adjacent Dinaridic ophiolite belt. Labeling DF2 is speculative due to low discriminant loadings but it possibly highlights the redox conditions controlling the trace-element enrichment-depletion in the bauxite-bearing palaeo-environment.

ACKNOWLEDGMENT

REFERENCES

ARRINDELL, W.A. & VAN DER ENDE., J. (1985): An empirical test of the utility of the observations-to-variables ratio in factor and components analysis.– Appl. Psych. Meas., 9, 165–178. doi:10.1177/014662168500900205

BANNING, A. & RÜDE, T.R. (2010): Enrichment processes of arsenic in oxidic sedimentary rocks - from geochemical and genetic characterization to potential mobility.– Water Res., 44, 5512–5531. doi:10.1016/j.watres.2010.05.034

BARDOSSY, G. (1982): Karst bauxites: bauxite deposits on carbonate rocks.– Akadémiai Kiadó, Budapest, 441 p.

BURTON, E.D., JOHNSTON, S.G. & BUSH, R.T. (2011): Microbial sulfidogenesis in ferrihydrite-rich environments: Effects on iron mineralogy and arsenic mobility.– Geochim. Cosmochim. Ac., 75, 3072–3087. doi:10.1016/j.gca.2011.03.001

CALAGARI, A.A. & ABEDINI, A. (2007): Geochemical investigations on Permo-Triassic bauxite horizon at Kanisheeteh, east of Bukan, West-Azarbaidjan, Iran.– J. Geochem. Explor., 94, 1–18. doi:10.1016/j.gexplo.2007.04.003

CHESTER, R. (1990): Marine Geochemistry.– Unwin Hyman, London, 689 p.

CHORLEY, R.J., SCHUMM, S.A. & SUGDEN, D.E. (1985): Encyclopedia of Geomorphology.– Routledge Publishing, 648 p.

CORBIN, J.C., PERSON, A., IATZOURA, A., FERRÈ, B. & RENARD, M. (2000): Manganese in Pelagic carbonates: indication of major Tectonic events during the geodynamic evolution of a passive continental margin (the Jurassic European Margin of the Tethys–Ligurian Sea).– Palaeogeogr., Palaeoclimat., Palaeoecol., 156, 123–138. doi:10.1016/S0031-0182(99)00135-2

CROATIAN GEOLOGICAL SURVEY (2009): Geološka karta Republike Hrvatske 1:300.000 [*Geological Map of the Republic of Croatia 1:300 000* – in Croatian].– Zagreb.

D'ARGENIO, B. & MINDSZENTY, A. (1995): Bauxites and related palaeokarst: tectonic and climatic event markers at regional unconformities.– Eclogae Geol. Helv., 88, 453–499.

DAVIS, J.C. (1986): Statistics and data analysis in geology.– John Wiley & Sons, New York, 646 p.

DE VOS, W., TARVAINEN, T. (Chief-editors), SALMINEN, R., REEDER, S., DE VIVO, B., DEMETRIADES, A., PIRC, S., BATISTA, M.J., MARSINA, K., OTTESEN, R.-T., O'CONNOR, P.J., BIDOVEC, M., LIMA, A., SIEWERS, U., SMITH, B., TAYLOR, H., SHAW, R., SALPETEUR, I., GREGORAUSKIENE, V., HALAMIĆ, J., SLANINKA, I., LAX, K., GRAVESEN, P., BIRKE, M., BREWARD, N., ANDER, E.L., JORDAN, G., DURIS, M., KLEIN, P., LOCUTURA, J., BEL-LAN, A., PASIECZNA, A., LIS, J., MAZREKU, A., GILUCIS, A., HEITZMANN, P., KLAVER, G. & PETERSELL, V. (2006): Geochemical Atlas of Europe. Part 2 – Interpretation of Geochemical Maps, Additional Tables, Figures, Maps, and Related Publications, Geological Survey of Finland, 690 p.

DILLON, W.R. & GOLDSTEIN, M. (1984): Multivariate analysis: methods and applications.– John Wiley & Sons, New York, 575 p.

DOORNKAMP, J.C. & KING, C.A.M. (1971): Numerical analysis in geomorphology: an introduction.– Edward Arnold, London, 368 p.

DRAGIČEVIĆ, I. & VELIĆ, I. (2002): The northeastern margin of the Adriatic Carbonate Platform.– Geol. Croat., 55/2, 185–232.

ECONOMOU-ELIOPOULOS, M. (2003): Apatite and Mn, Zn, Co-enriched chromite in Ni-laterites of northern Greece and their genetic significance.– J. Geochem. Explor., 80, 41–54. doi:10.1016/S0375-6742(03)00181-X

FORCE, E.R. (1991): Geology of Titanium-Mineral Deposits.– GSA Spec. Pap., 259, 112 p.

HALAMIĆ, J. & MIKO, S. (2009): Geochemical Atlas of the Republic of Croatia.– Croatian Geological Survey, Zagreb, 88 p.

HOSE, H.R. (1986): Mediterranean karst bauxite genesis and plate tectonics during the Mesozoic.– In: 4th International Congress for the Study of Bauxite, Alumina and Aluminum (ICSOBA), Athens. Proceedings, 333–341.

HUGGET, R.J. (1998): Soil chronosequences, soil development and soil evolution: a critical review.– Catena, 32, 155–172. doi:10.1016/S0341-8162(98)00053-8

HERRMANN, L., ANONGRAK, N., ZAREI, M., SCHULER, U. & SPOHRER, K. (2007): Factors and processes of gibbsite formation in Northern Thailand.– Catena, 71, 279–291. doi:10.1016/j.catena.2007.01.007

HIERONYMUS, B., KOTSCHOUBEY, B. & BOULÈGE, J. (2001): Gallium behaviour in some contrasting lateritic profiles from Cameroon and Brasil.– J. Geochem. Explor., 72, 147–163. doi:10.1016/S0375-6742(01)00160-1

HUERTA-DIAZ, M.A. & MORSE, J.W. (1992): Pyritization of trace metals in anoxic marine sediments.– Geochim. Cosmochim. Ac., 56, 2681–2702. doi:10.1016/0016-7037(92)90353-K

KETZER, J.M., MORAD, S. & AMOROSI, A. (2003): Predictive diagenetic clay-mineral distribution in siliciclastic rocks within a sequence stratigraphic network.– Int. Assoc. Sedimentol. Assoc. Spec. Publ., 34, 43–51.

KLEBER, M., SCHWENDENMANN, L., VELDKAMP, E., RÖSSNER, J. & JAHN, R. (2007): Halloysite versus gibbsite: silicon cycling as a pedogenetic process in two lowland neotropical rain forest soils of La Selva, Costa Rica.– Geoderma, 138, 1–11. doi:10.1016/j.geoderma.2006.10.004

KORBAR, T. (2009): Orogenic evolution of the External Dinarides in the NE Adriatic region: a model constrained by tectonostratigraphy of Upper Cretaceous to Paleogene carbonates.– Earth-Sci. Rev., 96, 296–312. doi:10.1016/j.earscirev.2009.07.004

KRUMBEIN, W.C. & GREYBILL, F.A. (1965): An introduction to statistical models in geology.– McGraw-Hill, Toronto-London-Sydney, 475 p.

MACLEAN, W.H. & BARRETT, T.J. (1993): Lithogeochemical techniques using immobile elements.– J. Geochem. Explor., 48, 109–133. doi:10.1016/0375-6742(93)90002-4

MATSCHULLAT, J., OTTENSTEIN, R. & REIMANN, C. (2000): Geochemical background – can we calculate it?– Environ. Geol., 39/9, 990–1000. doi:10.1007/s002549900084

MATIČEC, D., VLAHOVIĆ, I., VELIĆ, I. & TIŠLJAR, J. (1996): Eocene limestone overlying Lower Cretaceous deposits of Western Istria (Croatia): did some parts of present Istria form land during the Cretaceous?– Geol. Croat., 49/1, 117–127.

MERINO, E. & BANERJEE, A. (2008): Terra Rossa Genesis, Implications for Karst, and Eolian Dust: A Geodynamic Thread.– J. Geol., 116, 62–75. doi:10.1086/524675

ÖZLÜ, N. (1983): Trace element contents of karst bauxites and their parent rocks in the Mediterranean belt.– Miner. Deposita, 18, 469–476.

PALMER, M.R. (1985): Rare earth elements in foraminifera tests.– Earth Planet. Sc. Lett., 73, 285–298. doi:10.1016/0012-821X(85)90077-9

PAMIĆ, J., TOMLJENOVIC, B. & BALEN, D. (2002): Geodynamic and petrogenetic evolution of Alpine ophiolites from the central and NW Dinarides: an overview.– Lithos, 65, 113–142. doi:10.1016/S0024-4937(02)00162-7

PEH, Z. & HALAMIĆ, J. (2010): Discriminant function model as a tool for classification of stratigraphically undefined radiolarian cherts in ophiolite zones.– J. Geochem. Explor., 107, 30–38. doi:10.1016/j.gexplo.2010.06.003

PHILLIPS, J.D. (1999): Earth surface systems: complexity, order, and scale.– Blackwell, Malden, 180 p.

REIMANN, C. & FILZMOSER, P. (2000): Normal and lognormal data distribution in geochemistry: death of a myth. Consequences for the statistical treatment of geochemical and environmental data.– Env. Geol., 39/9, 1001–1014. doi:10.1007/s002549900081

REIMANN, C., FILZMOSER, P. & GARRET, R.G. (2005): Background and threshold: critical comparison of methods of determination.– Sci. Total Environ., 346, 1–16. doi:10.1016/j.scitotenv.2004.11.023

ROCK, N.M.S. (1988): Lecture Notes in Earth Sciences, 18: Numerical Geology.– Springer Verlag, Berlin, 427 p.

SAKAČ, K., ŠINKOVEC, B. & GABRIĆ, A. (1978): Geologija i paleogenski boksiti Moseć planine (Dalmacija, južna Hrvatska) [*Geological setting and bauxites of Mt. Moseć, Dalmatia (south Croatia) – in Croatian, with an English Abstract*].– Geol. vjesnik, 30/1, 199–218.

SAKAČ, K., ŠINKOVEC, B., JUNGWIRTH, E. & LUKŠIČ, B. (1984): Opća obilježja geološke građe i ležišta boksita područja Imotskog [*General characteristics of geological framework and bauxite deposits of Imotski area* - in Croatian].– Geol. vjesnik, 37, 153–174.

SAKAČ, K. & ŠINKOVEC, B. (1991): The bauxites of the Dinarides.– Travaux, 23, 1–12.

SHELDON, N.D. & TABOR, N.J. (2009): Quantitative paleoenvironmental and paleoclimatic reconstruction using paleosols.– Earth-Sci. Rev., 95, 1–52. doi:10.1016/j.earscirev.2009.03.004

StatSoft, Inc., 2006. STATISTICA (data analysis software system), version 7.1. www.statsoft.com

ŠEBEČIĆ, B., PALINKAŠ, L., PAVIŠIĆ, D., ŠEBEČIĆ, B. & TRUTIN, M. (1985): Bauxite occurrences in the region of Zavojane and northwardly of Imotski.– Geol. vjesnik, 38, 191–213.

ŠINKOVEC, B. (1973): The origin of Early Palaeogene bauxites of Istria, Yugoslavia.– Travaux, 3, 151–164.

ŠINKOVEC, B. & SAKAČ, K. (1981): Boksiti starijeg paleogene na otocima sjevernog Jadrana [*The Early Paleogene Bauxites of North Adriatic Islands* – in Croatian, with an English Abstract].– Geol. vjesnik, 33, 213–225.

ŠINKOVEC, B. & SAKAČ, K. (1991): Bauxite deposits of Yugoslavia – the state of the art.– Acta Geologica Hungarica, 34/4, 307–315.

ŠINKOVEC, B., SAKAČ, K. & DURN, G. (1994): Pyritized bauxites from Minjera, Istria, Croatia.– Nat. Croat., 3/1, 41–65.

ŠUŠNJARA, A., SAKAČ, K., GABRIĆ, A. & ŠINKOVEC, B. (1990): Boksiti područja Sinja u Srednjoj Dalmaciji [*Bauxites in the Sinj area in Middle Dalmatia* - in Croatian, with an English Abstract].– Geol. vjesnik, 43, 169–179.

TARDY, Y., TROLARD, F., EOQUIN, C. & NOVIKOFF, A. (1990): Distribution of hydrated and dehydrated minerals in lateritic profiles and landscapes.– In: Geochemistry of the Earth's surface and of mineral formation, 2nd International Symposium, July, 2–8, 1990, 133–136.

TAYLOR, S.R. & MCLENNAN, S.M. (1985): The Continental Crust: its Composition and Evolution.– Blackwell Scientific Publications, 312 p.

TIŠLJAR, J., VLAHOVIĆ, I., VELIĆ, I. & SOKAČ, B. (2002): Carbonate platform megafacies of the Jurassic and Cretaceous deposits of the Karst Dinarides.– Geol. Croat., 55/2, 139–170.

VALETON, I., BIERMANN, M., RECHE, R. & ROSENBERG, F. (1987): Genesis of nickel laterites and bauxites in Greece during the Jurassic and Cretaceous, and their relation to ultrabasic parent rocks.– Ore Geol. Rev., 2, 359-404. doi:10.1016/0169-1368(87)90011-4

VLAHOVIĆ, I., TIŠLJAR, J., VELIĆ, I. & MATIČEC, D. (2002): The Karst Dinarides are composed of Relics of a single Mesozoic Platform: Facts and Consequences.– Geol. Croat., 55/2, 171–183.

VLAHOVIĆ, I., TIŠLJAR, J., VELIĆ, I. & MATIČEC, D. (2005): Evolution of Adriatic Carbonate Platform: Palaeogeography, main events and depositional dynamics.– Palaeogeogr., Palaeoclimat., Palaeoecol., 220, 333–360. doi:10.1016/j.palaeo.2005.01.011